Electrochemical Kinetics and Mechanism of Hydrogen Absorption of Ti and Zr during Cathodic Electrolysis

Tadahiko MIZUNO* and Michio ENYO**

(Received September 9, 1993)

Abstract

Relationships between kinetics of hydrogen absorption by electrolysis and hydrogen concentration profiles of Ti and Zr were investigated by a nuclear chemical and other conventional technicqus. Hydrogen atoms interact very intensively with each others in the metal. Hydrogen concentration profiles were dependent on the condition of cathodic electrolysis and pre-treatment metal. A high level of hydrogen concentration in the surface layer was realized by electrolysis at high cathodic current density for a prolonged time. The rate of hydrogen absorption was influenced strongly by the formation of a layer having high hydrogen concentration.

1. Introduction

Effects of surface hydride layer on the hydrogen absorption are of interested in connection with the hydrogen evolution kinetics. However, a limited number of investigations have been carried out on the hydrogen behaviour during cathodic electrolysis. Hydrogen absorption phenomena have a great importance in practice, and it recently has gained renewed interests in relation with alleged Cold Fusion phenomena. The phenomena are still in dispute because of the difficulties in reproducibility and lack of information on the mechanism. Few technique can be considered to induce the Cold Fusion reaction; one of then is the main to the reaction induce by electrolysis and other is the gas fill up technique.

Hydrogen evolution may take place according to the following mechanism;

$$H^+ + e^- \rightarrow H_{ads} \quad (1)$$

$$H_{ads} + H_{ads} \rightarrow H_2 \quad (2)$$

The mechanism has been discussed by Bockris[1], Parsons[2], Thomas[3] and Conway[4]. A part of adsorbed hydrogen atoms H_{ads} are absorbed and diffuse into metals, often forming hydride phases.

The following factors may control the reaction of hydrogen absorption,

(1) Mehanism of the hydrogen electrode reaction
(2) Effect of impurities in the solution upon rate controlling natnre of elementary steps
(3) Surface concentration/activity of hydrogen adatoms
(4) Energetics of the $H_{ads} \rightarrow H_{abs}$ reaction

* Dept. Nuclear Engineering
** Catalysis Research Center

(5) hydride layer

2. Experimental

2. 1 Evaluation of total amount of hydrogen in metal

The total amount of hydrogen absorbed in a metal or a metal hydride sample can be estimated by conventional methods such as direct weighing[5,6], QCM (quartz crystal microbalance)[7,8], observation of expansion of the metal specimen[9], or of hydrogen gas which is released upon heating invacuum, etc. Hydrogen can be expelled from exothermic hydrogen absorbing metals, typically Pd, by heating. In the case of Ti, hydride may be decomposed by heating to 1,000 K, and the amount of hydrogen measured precisely by means of a volumetric technique[10-13]. The etching solution was chosen so that it should provide relatively mild dissolution rate of the hydride layer and no additional production of hydrogen should take place during the etching treatment. A mixed solution of 1.2 wt. % HF+2.0 wt. % HNO_3 was found suitable for Ti hydride or 1.0 wt. % HF+2.0 wt. % H_2O_2 for Zr hydride[14].

2. 2 Hydrogen concentration profile

The hydrogen concentration profile in the bulk metal near its surface is an interesting quantity at the time when the hydrogen distribution in metal has not yet attained homogeneous distribution because of diffusional limitations. This would provide information on the mobility of hydrogen in the metal. In the case of Zr and Ti, the concentration profile could be measured by a differential etching technique: The sample metal is gradually dissolved in an etching solution and the hydrogen gas released is collected and its volume measured. The thickness resolution of the hydrogen concentration profile in this technique is of the order of 10^{-5}cm[15].

2. 3 Analysis of deuterium in metal by the d-n reaction using a deuteron accelerator

It is very important to trace in detail the process of hydrogen absorption into the surface layer of a metal in order to understand detailed mechanism of hydrogen permeation. Conventional techniques such as the one described above are only approximate in elucidating the concentration profile or to evaluate the rate of hydrogen absorption in a thin layer of hydrogen absorbing metals.

A d-n (d: deuteron, n: neutron) nuclear chemical method of analysis of deuterium absorbed in metal by deuteron bombardment using an accelerator was developed. Neutrons evolved by a nuclear fusion reaction that took place were measured and the deuterium concentration in the sample surface layer was estimated therefrom. The sample surface is dissolved stepwise by etching and then subjected to the d-n reaction analysis, but with use of the deuteron beam energy which is lowered by one to two orders of magnitude (1~10 keV) so that the penetration depth of deuteron into the sample was decreased to the order of 10^{-4}~10^{-6}cm. In this way, the thickness resolution was brought to as low as 10^{-7}cm. Analysis of the relationship between the rate of neutron evolution and the incident deuteron beam energy may thus provide a fine deuterium concentration profile in the sample metal. Further, this method has an

important application to the study of isotope effects between H and D, as will be presented later.

3. Experimental results

3. 1 Kinetics of hydrogen absorption

The behavior of hydrogen absorption in Ti and Zr by electrolysis is probably similar as that with Pd. On these electrodes, formation of a layer at the electrode surface with very high hydrogen concentration, which retards the rate of hydrogen absorption, is suggested especially at high c. d. of electrolysis or after long time charging.

Cathodic c. d. influences on the nature and rate of the hydrogen absorption in Ti and Zr. Figure 1 shows log-log plot of the time dependence of the amount of hydrogen accumulated in Zr at various cathodic c. d. in 1 N Na_2SO_4 at 303 K. It shows that, although the rate of absorption increases with c. d., the inclination of the hydrogen absorption curves decreases with increase of amount of the hydrogen aptake of the electrode; rate of the hydrogen absorption obeys a linear rate law at amounf of hydrogen uptake of the electrode lower than 5 mA cm^{-2} (namely, the slope is unity) but it changes to a parabolic law at the higher c. d.(slope is 1/2).

Analogous results are obtained for Ti in 1 N H_2SO_4. The kinetics of hydrogen absorption obeys a linear rate law at the beginning of cathodic polarization at various c. d.'s, but it changes to a parabolic law after the sample absorbed roughly 0.3 cm^3 volume hydrogen per unit area (H/Zr=1.0).

Rise in temperature accelerates the hydrogen absorption rate[16]. The rate laws are different at different current densities . Nevertheless the activation energy values for hydrogen absorption are practically the same with each other, being~17 kJ mol^{-1}. The corresponding value for Zr was ~17 kJ mol^{-1}. It seems that the value is not dependent on the condition of cathodic polarization; the time dependence of hydrogen absorption

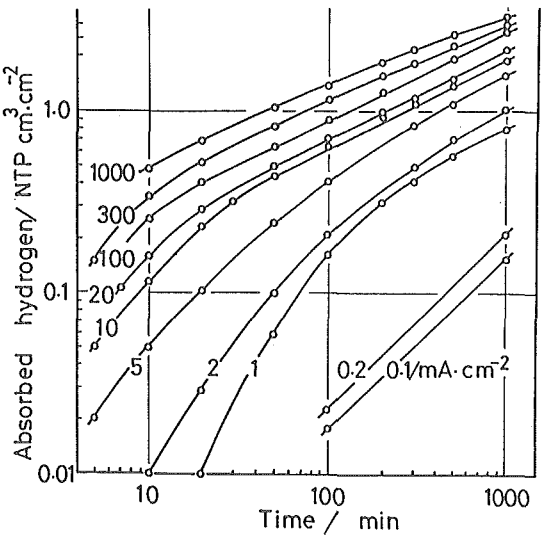

Fig. 1 Effect of cathodic current density on hydrogen absorption of Zr in 0.5 N Na_2SO_4 at 30℃

is mainly controlled by the rate of diffusion in the metal.

The activation energy of the phase transformation is 40 kJ·mol^{-1} and the hydrogen content is strongly dependent on the cathodic c. d.. If the hydrogen absorption process is controlled by the diffusion, the value is expected to 40~50 kJ. mole^{-1}. Experimental results indicate that the hydrogen absorption process is controlled by other reaction such as the phase transformation and the surface reaction.

The pH change gives rise to a significant difference in the hydrogen absorption into Ti. Thus, the absorption takes place readily at low pH values, but not significantly at high pH. On the other hand, hydrogen absorption into Zr takes place in the whole range of pH. Figure. 2 shows effects of pH and of presence of alkali metal ions upon the hydrogen absorption rate into Zr. The rates show a maximum around neutral pH region, and alkali metal ion appears to accelerate the rate of hydrogen absorption. Decrease of hydrogen absorption rate at low pH may mean improved rate of hydrogen recombination reaction on Zr, which provides easier path of hydrogen escape. Similar increase of the absorption rate is also seen in the presence of Na^+ and K^+. It may be possible that they suppress the rate of recombination reaction between, and thus raising the activity of, hydrogen adatoms.

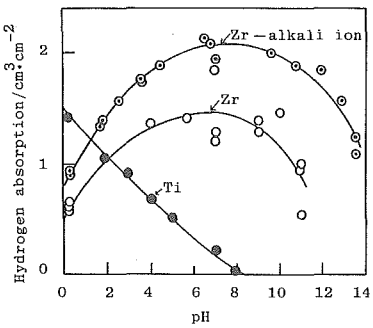

Fig. 2 Effect of pH and existence of alkali metal ion on the hydrogen absorption into Zr

3. 2 Hydrogen Concentration Profile in Ti and Zr Hydride

The hydrogen concentration profile obtained in Ti by a volumetric technique has indicated a sigmoid shape as shown in Fig. 3a, with the detail being dependent on the cathodic c. d. It gives a clear plateau region after a long time of cathodic polarization, e. g., 6×10^4 s at c. d. of 10 mA cm^{-2} in 1 N H_2SO_4. The H/Ti ratio at the plateau increases with the c. d. The sigmoid shape of the concentration profile clearly indicates that hydrogen in Ti is not of simple sorption controlled by diffusion, but formation of a hydride layer near the surface with the hydrogen content of H/Ti~1.5 and it progresses towards bulk of the Ti specimen, with increasing rate at higher c. d. or temperature.

Formation of similar hydride layer is also indicated in Zr (Fig. 3b). The hydrogen concentration profiles generally have a sigmoid shape, having a plateau which becomes thicker and clearer with increase of c. d. and of duration of time. Structural analysis at each points numbered in these figures indicated that structures are changing with

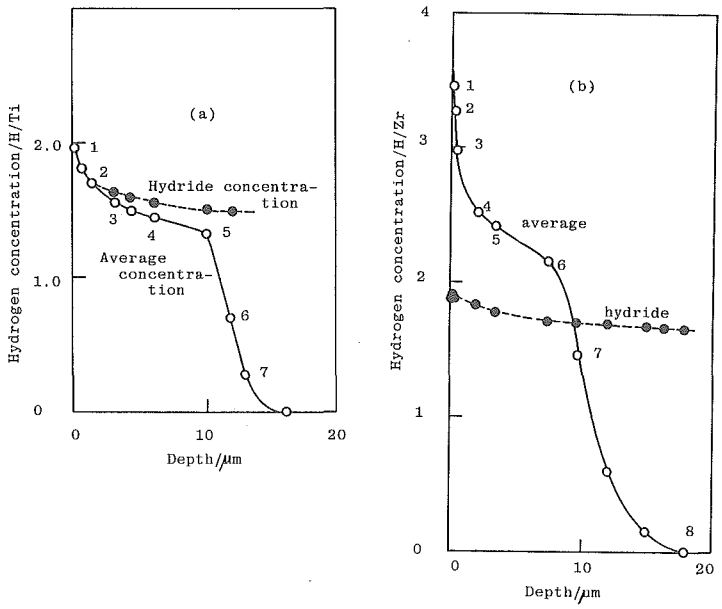

Fig. 3 Hydrogen concentration profiles in bilk and hydride phase of Ti, (a) and Zr, (b).

Table 1 Composition, structure and lattice parameters of Ti and Zr hydride at various positions numbered in Fig. 3

No.	Corrmp. (x)	Structure	Lattice parameter
	Ti		
	TiH_x		
1	2.0	fct(ε)	a=4.44
2	1.71	fcc(δ)	a_0=4.42
3	1.54	〃	4.41
4	1.45	fcc+hcp(α)	4.41
5	1.33	〃	〃
6	0.72	〃	〃
7	0.30	〃	〃
	Zr		
	ZrH_x		
1	3.45	fct(ε)	a=4.960, c=4.47
2	3.27	〃	4.98, 4.48
3	2.98	ε+fcc(δ)+hcp(α)	4.96, 4.48, a_0=4.80
4	2.52	〃	4.95, 4.48, 4.80
5	2.42	〃	4.92, 4.53, 4.78
6	2.16	〃	4.90, 4.70, 4.78
7	1.47	$\delta+\alpha$	4.78
8	0	α	

change of the hydride composition, as given in Table 1. It was seen on Ti that both α- and δ-Ti-H are formed from the beginning of the hydride formation. The composition of the δ-phase is almost constant, being $TiH_{1.5-1.54}$, but it increases further after disappearance of α-phase. The hydrogen concentration profiles in the δ-Ti-H hydride

phase are also shown in Fig. 3 which agree with the data by volumetric method only at the surface.

The composition at a very thin surface layer can be obtained by the d, n method; typical results are shown in Fig. 4 It is seen that the absorption of hydrogen (deuterium) increases almost linearly with time at the beginning. This, together with the behavior quoted above, may indicate that at the beginning of hydride phase having a constant concentration grows with time until the α-phase is completed. The final hydrogen concentration in the surface layer finally reaches D/M≃2.0 for Ti but it is still increasing at Zr.

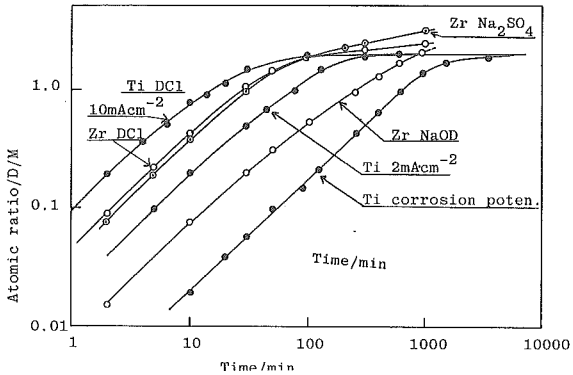

Fig. 4 Composition at the surface layer obtained by the d, n method.

3. 3 Microscopic observation of growth of hydride layer

SEM observations of surface hydride layer formed by cathodization of Ti are shown in Fig. 5 The hydride layer consists of two portions, uniform hydride layer and a layer of needle/wedge-like structure which is intruding into bulk of the metal. Such a structure is formed from the beginning with a thin needle-like shape but they gradually grow both in length and width which may reach 2~3 μm. The cross section view of the wedge-like portion is shown in Fig. 6 which indicates hydrided portion (black) and α-Ti phase (white).

The progress of hydride formation in metals may be summarized as follows: (1) at the beginning, thin needle-like hydride structure is formed, which is δ-phase for Ti and δ and ε-phase for Zr, (2) the needles grow thicker and tend to merge with each other; the phase gradually becomes one phase of δ for Ti and ε for Zr, (3) the surface layer becomes plate-like uniform structure, and (4) hydrogen concentration in the plate-like hydride gradually grows and finally reaches stoichiometric composition: these are schematically shown in Fig. 7.

3. 4 Further details of hydrogen absorbed layer as studied by the d-n reaction method

A more detailed behavior or hydrogen absorption can be obtained by the combining etching/volumetric method described before with the d-n analysis. Specimen is first polarized in light water solution followed by polarization in heavy water solution, or

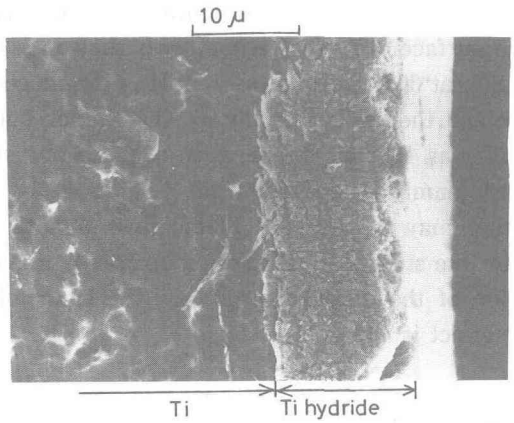

Fig. 5 SEM observation of hydride layer on Ti.

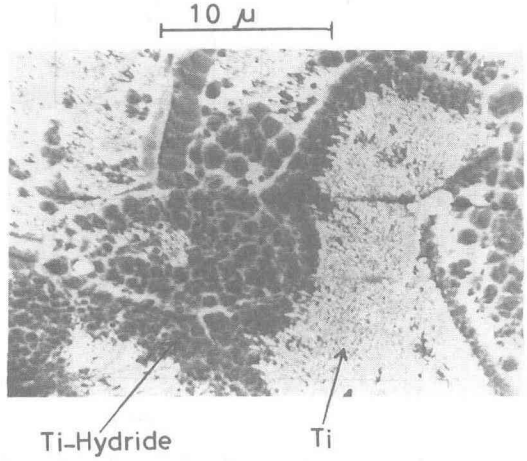

Fig. 6 SEM observation of the cross sectional view of the wedge like portion in Fig. 5.

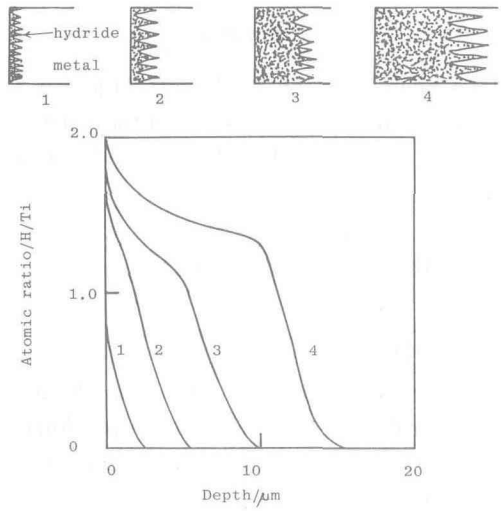

Fig. 7 Schematical representation of hydride formation process and the concentration profiles.

reverse order, and both hydrogen content and deuterium concentration are evaluated at various depth from the surface. Typical results are shown in Fig. 8 for Zr which is polarized in 0.5 M Na_2SO_4 at 30℃ as follows: (a) H is introduced first to form hydride of needle-like structure and then D is introduced, (b) similar but the reverse order, H into deuteride, (c) Similar as (a) but for the case of plate-like structure, and (d) similar but the reverse order, namly H ioto deuteride.

The following picture may be drawn: (1) mobility of both H and D is larger in needle-like than in plate-like structure, (2) H is more easily moved by D than for D by H, (3) heat of activation of the diffusion process is ~49 kJ mol^{-1} both for H and D, and (4) kinetic isotope effect is~14.4[17].

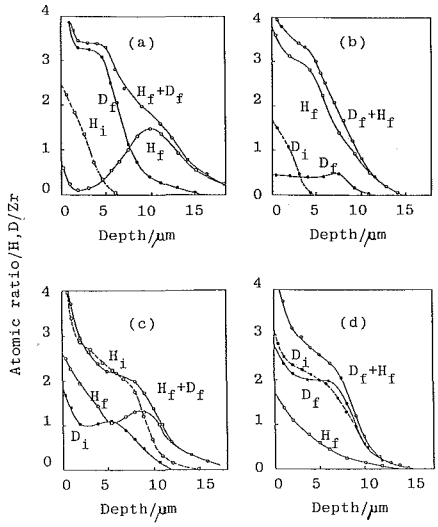

Fig. 8 Movement of hydrogen and deuterium in needle and plate like hydride layer.

4. Discussion

Various attempts have been reported in the literature to account for the relation between hydrogen absorption into cathode metal and the condition of the cathodization. Thus, Bockris, McBreen and Nanis (BMN)[18] proposed the following Volmer-Tafel scheme,

$$H_3O^+ + e^- + M \xrightarrow{k_1} MH_{ads} \xrightarrow{k_3} M + (1/2)H_2 \tag{3}$$

$$k_3 \uparrow\downarrow k_{-3}$$

$$MH_{ads} \tag{4}$$

One may assume that the hydrogen absorption rate J at the begining of hydrogen entry or with low hydrogen concentration in the metal is proportional to hydrogen concentration C immediately beneath the surface and further that the latter is proportional to the activity a_{ads} of H_{abs}, namely,

$$J = k_4 C = k_5\ a_{abs} \tag{5}$$

The electrolysis current i written for Tafel step may be given by

$$i=k_2(a_{abs})^2 \quad (6)$$

It then follows

$$J=k_2k_5\, i^{1/2} \quad (BMN) \quad (7)$$

On the other hand, Bagotskaya and Frumkin (BF)[19] adopted the scheme which assumes direct entry of hydrogen, namely,

$$H_3O^+ + e^- + M \longrightarrow MH_{abs} \longrightarrow M + (1/2)H_2 \quad (8)$$

$$\updownarrow$$

$$MH_{ads} \quad (9)$$

One may then take,

$$a_{abs}=k_6 \exp(-F\eta/RT) \quad (10)$$

Also, looking at Volmer step,

$$i=k_7 \exp(-\alpha F\eta/RT) \quad (11)$$

hence, one obtains from Eqs.(5) and (11), with $\alpha=1/2$,

$$J=k_5k_6i^2 \quad (BF) \quad (12)$$

According to the observation in this work on Ti and Zr, however, it was seen that the J *vs.* i relation, or the order of reaction, was close to unity at low hydrogen content, thus in agreement with neither of these predictions, 1/2 or 2.

On the other hand, it appears reasonable to have the reaction order around unity as

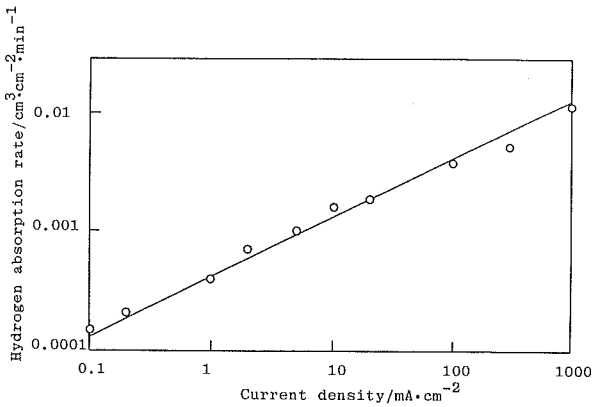

Fig. 9 Relationship between hydrogen absorption rate and current density of Zr.

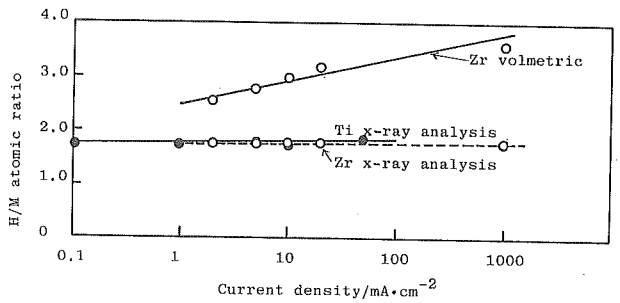

Fig. 10 Hydrogen concentration at the surface layer obtained by x ray analysis and volumetric measurement.

based on a general analysis with a mixedcontrolled model[20]. On Pd and Fe electrode, the effective hydrogen pressure was deduced to depend on η with the slope of approximately 120~150 mV/decade, being not significantly dependent on kinetic parameter values. As the Tafel slope on these metals in the range of η concerned is generally ~120 mV, the dependence of the effective pressure upon polarization current i should come out to be about unity order. Detailed analysis will be reported separately[21].

The order generally tends to decrease to 0.5 or lower at higher hydrogen concentration. This is probably due to gradual approach to saturation of hydrogen at least in the region close to the surface which would retard further hydrogen absorption.

5. Conclusions

Direct observation to the hydride formation process for Ti and Zr show following results:

(1) Mechanism of hydrogen evolution shows the intermediate relationship of BBN and BF before the surface was covered with the hydride.
(2) The BBN mechanism is held after the surface was covered with the hydride layer.
(3) Rate of hydrogen absorption show linear relationship at the beginning of cathodic electrolysis, and show protective film law as increase of hydride layer.
(4) Hydride phase change from δ to ε with increase of hydride layer.
(5) Hydrogen content exceed the stoichiometric value of 2 with long and strong cathodic polarization for Zr while it stays under the value of 2.0 for Ti.

6. References

1. J. O' M. Bockris, M. A. Genshow and M. Fullenwider; Electrochem. Acta., 15 (1970) 47-60.
2. Parsons; Trans. Faraday Soc., 54 (1958) 1053.
3. J. G. N. Thoman; Trans. Faraday Soc., 57 (1961) 1603~1611.
4. B. E. Conway; M. Salomon; Electrochemica. Acta., 9 (1964) 1599~1615.
5. M. A. V. Devanathan, J. O' M. Bockris, and W. Mehl; J. Electroanal. Chem., 1 (1989/60) 143.
6. P. K. Iyengar; Proc. Fifth Int. Conf. on Emerging Nuclear Energy Systems, Karlsruhe (1984).
7. N. Yamamoto, T. Ohsaka, T. Terashima and N. Oyama; J. Electroanal. Chem., 296 (1990) 463.
8. L. Grasjo and M. Seo; J. Electroanal. Chem., 296 (1990) 233.
9. H. Numata and I. Ohno; 183-rd ECS Meeting, Hawaii, May 16-21 (1993), No. 1772.
10. T. B. Flanagan and F. A. Lewis; Trans. Faraday Soc., 55 (1959) 1400, 1409.
11. J. C. Barton and F. A. Lewis; Talanta, 10 (1963) 237.
12. J. Sshirber and C. Northrup Jr; Phys. Rev., B10 (1976) 3818.
13. N. Lewis, C. Barnes, M. Heben, A. Kumar, S. Lunt, G. McManis, G. Milkelly, R. M. Penner, P. Santangelo, G. Shreve, B. Tufts, M. Youngquist, R. Kavanagh, S. Kellogg, R. Vogelaar, T. Wang, R. Kondrat and R. New; Nature, 340 (1989) 525.
14. T. Mizuno and T. Morozumi; Bullletin Faculty of Eng. Hokkaido Univ., No. 93 (1979) 23.
15. T. B. Flanagan and F. A. Lewis; Z. Physik. Chem. (N. F.), 27 (1961) 104.
16. T. Mizuno, T. Shindo and T. Morozumi; Boshoku Gijutsu, 26 (1977) 185.
17. T. Mizuno; J. Japan Inst. Metals., 55 (1991) 553.
18. J. O'M. Bockris, J. McBreen and L. Nanis; J. Electrochem. Soc., 112 (1965) 1025.
19. Z. A. Bagotskaya and A. N. Frumkin; Z. Fiz. Khim., 32 (1962) 2677.
20. M. Enyo, Comprehensive Treatise of Electrochemistry, No. 7, ed. by B. E. Conway et al., Plenum, New York, (1983) 241.

21. M. Enyo, to be published.